

Understanding and improving the reusability of phosphate adsorbents for wastewater effluent polishing

Suresh Kumar, Prashanth; Ejerssa, Wondesen Workneh; Wegener, Carita Clarissa; Korving, Leon; Dugulan, Achim Iulian; Temmink, Hardy; van Loosdrecht, Mark C.M.; Witkamp, Geert Jan

DOI

[10.1016/j.watres.2018.08.040](https://doi.org/10.1016/j.watres.2018.08.040)

Publication date

2018

Document Version

Accepted author manuscript

Published in

Water Research

Citation (APA)

Suresh Kumar, P., Ejerssa, W. W., Wegener, C. C., Korving, L., Dugulan, A. I., Temmink, H., van Loosdrecht, M. C. M., & Witkamp, G. J. (2018). Understanding and improving the reusability of phosphate adsorbents for wastewater effluent polishing. *Water Research*, 145, 365-374. <https://doi.org/10.1016/j.watres.2018.08.040>

Important note

To cite this publication, please use the final published version (if applicable). Please check the document version above.

Copyright

Other than for strictly personal use, it is not permitted to download, forward or distribute the text or part of it, without the consent of the author(s) and/or copyright holder(s), unless the work is under an open content license such as Creative Commons.

Takedown policy

Please contact us and provide details if you believe this document breaches copyrights. We will remove access to the work immediately and investigate your claim.

1 Understanding and improving the reusability of phosphate adsorbents
2 for wastewater effluent polishing

3 Prashanth Suresh Kumar^{a,b*}, Wondesen Workneh Ejerssa^a, Carita Clarissa Wegener^c, Leon Korving^{a*},
4 Achim Iulian Dugulan^d, Hardy Temmink^{a,e}, Mark C.M. van Loosdrecht^b, Geert-Jan Witkamp^{b,1}

5 ^aWetsus, European Centre Of Excellence for Sustainable Water Technology, Oostergoweg 9, 8911 MA,
6 Leeuwarden, The Netherlands

7 ^bDepartment of Biotechnology, Applied Sciences, Delft University of Technology, Building 58, Van der
8 Maasweg 9, 2629 HZ Delft, The Netherlands

9 ^cChair for Mechanical Process Engineering / Water Technology, Faculty of
10 Engineering, University Duisburg-Essen, Lotharstrasse 1, 47057 Duisburg,
11 Germany

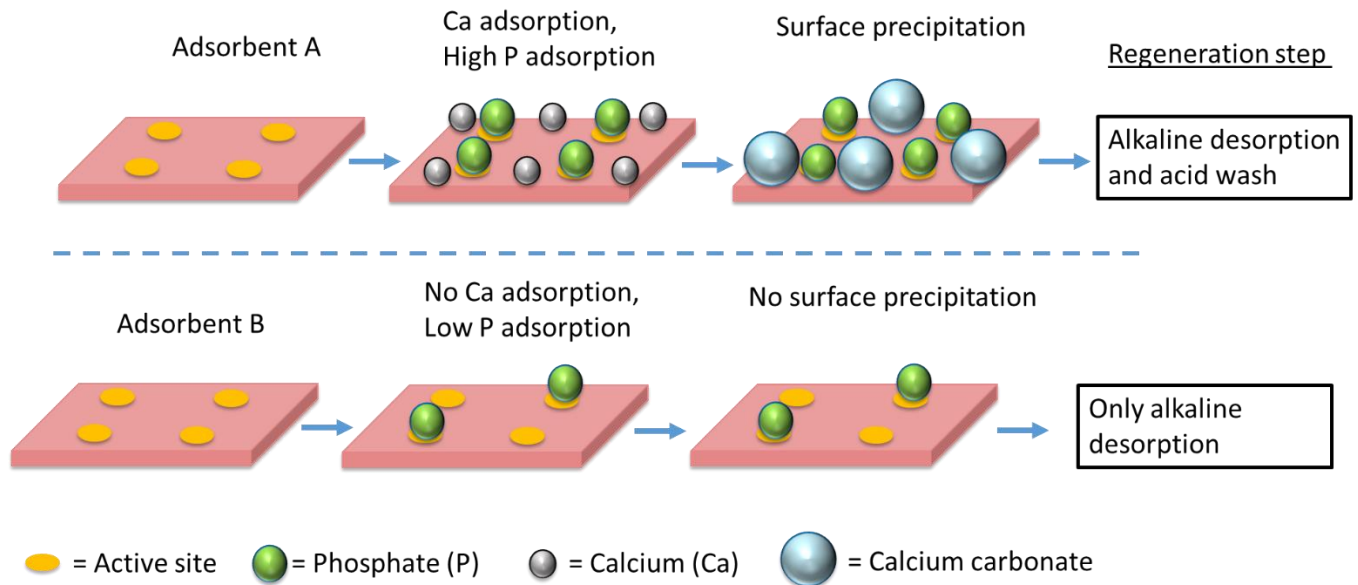
12 ^dFundamental Aspects of Materials and Energy Group, Delft University of Technology, Mekelweg 15,
13 2629 JB Delft, The Netherlands

14 ^eSub-department of Environmental technology, Wageningen University and Research, Bornse Weiland
15 9, 6708 WG, Wageningen, The Netherlands.

16 ¹Current address: King Abdullah University of Science and Technology (KAUST), Water Desalination and
17 Reuse Center (WDRC), Division of Biological and Environmental Science and Engineering (BESE), Thuwal,
18 23955-6900, Saudi Arabia.

19 *Corresponding author: psureshkumar@tudelft.nl; Department of Biotechnology, Applied Sciences, Delft
20 University of Technology, Building 58, Van der Maasweg 9, 2629 HZ Delft, The Netherlands

21 Graphical abstract



22

23 Abstract

24 Phosphate is a vital nutrient for life but its discharge from wastewater effluents can lead to
25 eutrophication. Adsorption can be used as effluent polishing step to reduce phosphate to very low
26 concentrations. Adsorbent reusability is an important parameter to make the adsorption process
27 economically feasible. This implies that the adsorbent can be regenerated and used over several cycles
28 without appreciable performance decline. In the current study, we have studied the phosphate
29 adsorption and reusability of commercial iron oxide based adsorbents for wastewater effluent. Effects
30 of adsorbent properties like particle size, surface area, type of iron oxide, and effects of some competing
31 ions were determined. Moreover the effects of regeneration methods, which include an alkaline
32 desorption step and an acid wash step, were studied. It was found that reducing the adsorbent particle
33 size increased the phosphate adsorption of porous adsorbents significantly. Amongst all the other
34 parameters, calcium had the greatest influence on phosphate adsorption and adsorbent reusability.
35 Phosphate adsorption was enhanced by co-adsorption of calcium, but calcium formed surface

36 precipitates such as calcium carbonate. These surface precipitates affected the adsorbent reusability
37 and needed to be removed by implementing an acid wash step. The insights from this study are useful in
38 designing optimal regeneration procedures and improving the lifetime of phosphate adsorbents used for
39 wastewater effluent polishing.

40 **Key words:** Phosphate adsorption, wastewater effluent, regeneration, reusability, surface precipitation,
41 calcium adsorption

42 1. Introduction

43 Phosphate, the common form of inorganic phosphorous, is a vital nutrient for life and an essential
44 component of food. Humans consume phosphate as food which subsequently ends up in municipal
45 wastewater plants (Cordell et al. 2009). Discharge of phosphate from the wastewater effluent even in
46 the range of micrograms per liter can cause eutrophication of surface water (L. Correll 1998). Adsorption
47 is often suggested as a polishing step but for the process to be economically feasible, either the
48 adsorbent needs to be extremely cheap or be reusable (Li et al. 2016, Loganathan et al. 2014). Effective
49 reusability means the adsorbent can be regenerated and used again for several cycles without
50 diminishing its adsorption capacity. The reusability of the adsorbent via regeneration also enables
51 phosphate recovery and contributes to a circular economy.

52 Many studies focus on producing phosphate adsorbents with high adsorption capacity but fewer studies
53 touch on the reusability aspect (Li et al. 2016). An adsorbent's performance can decrease over time due
54 to multiple reasons. These include incomplete desorption of adsorbate, surface precipitation, loss of
55 active sites due to adsorbent wear and tear, and changes in adsorbent properties like surface area,
56 porosity, crystallinity during adsorption and regeneration (Cabrera et al. 1981, Chitrakar et al. 2006,
57 Kunaschk et al. 2015). The reusability of the adsorbents becomes an issue especially in a complex matrix
58 like wastewater effluent where several ions can bind simultaneously on the adsorbent. Thus the choice

59 of regeneration procedure is important in ensuring proper release of the bound ions. For instance, metal
60 oxides like iron (hydr)oxides bind phosphate via a ligand exchange mechanism with their surface
61 hydroxyl groups (Cornell and Schwertmann 2004). Their regeneration requires using an alkaline solution
62 to reverse the reaction and release the bound phosphate (Kalaitzidou et al. 2016). However, an earlier
63 study showed surface precipitation on iron oxide adsorbents used in a drinking water matrix and an
64 additional step using acidic solution was required to regenerate the adsorbents (Kunaschk et al. 2015).
65 Moreover, regeneration first with an acidic solution before using alkaline solution improved the
66 adsorbent reusability compared to the reverse order. This was attributed to surface precipitates
67 blocking the adsorbed phosphate and hence the need to first remove the surface precipitates before
68 desorbing the phosphate.

69 In the current study, we use a similar regeneration approach to optimize phosphate adsorbents in
70 municipal wastewater effluent. We used commercially available iron (hydr)oxide based adsorbents since
71 iron oxides have been known for their good phosphate adsorption properties (Cornell and Schwertmann
72 2004). These were granular ferric hydroxide (GEH), Ferrosorp (FSP), and an ion exchange resin
73 impregnated with iron oxide (BioPhree). GEH and FSP are porous iron oxides chosen for their high
74 surface area. The BioPhree (henceforth referred as IEX) is similar to a hybrid ion exchange resin where
75 the iron oxide is responsible for the phosphate adsorption and the resin acts as a backbone matrix
76 (Blaney et al. 2007). Two principal factors of an adsorbent govern the process economics: i) Its
77 adsorption capacity (at a given effluent concentration and under a given operation time) ii) its
78 reusability. During the course of the experiments, we focused on improving both these properties. The
79 regeneration procedure used included an alkaline solution to desorb phosphate as well as an acidic
80 solution to remove surface precipitates. The order of using these solutions was also varied during
81 regeneration to understand the effect on reusability. Moreover, adsorbent properties (like surface area
82 and crystallinity) and mass balances of competing ions were monitored during the different adsorption-

83 regeneration cycles. Finally, to test adsorbent regeneration from a practical viewpoint, a regeneration
84 process with a minimal number of steps and chemical consumption was done. The methods were aimed
85 at monitoring the adsorbents to develop the best practices to regenerate and reuse the adsorbents.

86 2. Materials and methods

87 2.1. Chemicals

88 Potassium dihydrogen phosphate (KH_2PO_4), hydrochloric acid (HCl) and sodium hydroxide (NaOH) were
89 obtained from VWR chemicals. The adsorbents: granular ferric hydroxide (GEH), Ferrosorp (FSP) and ion
90 exchange resin impregnated with iron oxide (commercially called BioPhree, but referred to as IEX
91 henceforth) were provided by GEH Wasserchemie GmbH, HeGO Biotech GmbH, and Green Water
92 Solution, respectively.

93 2.2. Methods

94 2.2.1. Wastewater effluent

95 Wastewater effluent was sampled from Leeuwarden wastewater treatment plant and spiked using
96 KH_2PO_4 to get an initial phosphate concentration around 2 mg P/L. No other chemicals were spiked. The
97 particulates in the wastewater effluent were separated by sedimentation and only the supernatant was
98 used for the adsorption runs. Phosphorous analysis of filtered (using 0.45 μm membrane filter) and
99 unfiltered supernatant showed that there was no particulate phosphorus larger than 0.45 micron
100 present in the supernatant.

101 2.2.2. Adsorbent columns

102 Adsorbents GEH and FSP were ground and sieved to reach particle size ranges of 1 to 1.25 mm and 0.25
103 to 0.325 mm, respectively. IEX was by default delivered (in its wet state) in the particle size range
104 between 0.25 to 0.325 mm. The adsorbents were filled inside a glass column (height = 20 cm, diameter =

105 1.8 cm) to get an adsorbent bed volume of 10 ± 0.5 ml. The adsorbent bed was packed by using glass
106 wool and glass beads to fill the remaining volume of the column (fig S1 in supporting information shows
107 the adsorbent column).

108 2.2.3. Adsorption and regeneration experiments

109 For the adsorption experiments, the wastewater effluent was pumped to the adsorbent columns in an
110 upflow mode with a flowrate of 2 ml/min. This gave an empty bed contact time (EBCT) of 5 minutes. The
111 treated solution from the outlet of the column was collected in an automated fraction collector every 3
112 to 5 hours. These were analyzed for phosphate and the adsorption process was stopped when the outlet
113 phosphate concentration reached 0.1 mg P/L.

114 Adsorbent regeneration was done in different ways. The first method, designated as alkaline-acid
115 regeneration, used an alkaline solution followed by an acidic solution. The second method, designated
116 as acid-alkaline regeneration, used acidic solution followed by alkaline solution. In both these methods,
117 the acid wash was done till the pH coming out of the column matched the initial pH of the acid solution.
118 Moreover the pH in the adsorbent column was neutralized with distilled water or HCl solution of pH 4
119 prior to subsequent adsorption cycles. Finally, in another method, the adsorbent was regenerated only
120 with alkaline solution and the pH in the adsorbent column was not neutralized prior to subsequent
121 adsorption cycles. Table 1 summarizes the different regeneration methods used. For all methods, 3
122 adsorption and regeneration cycles were done. The GEH and FSP adsorbent particle sizes were varied to
123 check the influence on the adsorption capacity, whereas the IEX was only available in the size range of
124 0.25 to 0.325 mm. The rationale for varying the acid wash conditions in different regeneration cycles
125 was to improve the reusability. The terms alkaline desorption and acid wash are used in the text to
126 imply release of ions from the adsorbent using alkaline and acidic solution respectively.

127

128 **Table 1:** Differences in the regeneration methods

Regeneration method	Adsorbents used	Particle size (mm)	Regeneration conditions
Alkaline-acid regeneration	GEH, FSP	1 to 1.25	<p><u>Alkaline desorption –</u></p> <p>For all 3 cycles: 100 ml of 1 M NaOH, Recirculation mode for 24 h, Flowrate = 5 ml/min;</p> <p><u>Acid wash -</u></p> <p>For all 3 cycles: Single pass mode with HCl (pH = 4) till outlet pH reached 4, Flowrate= 2 ml/min</p>
Acid-alkaline regeneration	GEH, FSP, IEX	0.25 to 0.325	<p><u>Acid wash –</u></p> <p>1st cycle: Recirculation mode with 1L HCl (pH = 4), HCl was added to the acid reservoir till pH stabilized at 4. 2nd and 3rd cycle: HCl (pH = 2.5), Single pass mode till outlet pH reached 2.5, Flowrate = 2ml/min;</p> <p><u>Alkaline desorption –</u></p> <p>For all 3 cycles: 100 ml of 1 M NaOH, Recirculation mode for 24 h,</p>

			Flowrate = 5 ml/min
Alkaline regeneration	FSP	0.25 to 0.325	<u>Alkaline desorption</u> For all 3 cycles: 100 ml of 1 M NaOH, Recirculation mode for 24 h, Flowrate = 5 ml/min

129

130 2.2.4. Analysis of wastewater samples

131 Calcium, magnesium, nitrate, nitrite, phosphate and sulphate ions were analyzed by ion
132 chromatography (Metrohm Compact IC Flex 930). Soluble phosphorous, silicon, and iron were measured
133 using inductively-coupled plasma optical emission spectroscopy (Perkin Elmer, Optima 5300 DV).
134 Dissolved organic carbon and inorganic carbon (carbonate ion) were measured using combustion
135 catalytic oxidation method with TOC analyzer (Shimadzu, TOC-L CPH). Table 2 shows the composition of
136 the wastewater effluent used.

137 **Table 2:** Wastewater effluent (from Leeuwarden) characteristics:

Components/Parameters	Average value/concentration
Temperature (during adsorption)	21 °C
pH	7.9 ± 0.2
Conductivity	1.8 ± 0.2 mS/cm
Calcium	66 ± 5 mg Ca/L
Magnesium	17 ± 0.5 mg Mg/L

Nitrate	5.5 ± 1 mg NO ₃ ⁻ /L
Nitrite	2.5 ± 2 mg NO ₂ ⁻ /L
Phosphate (after spiking)	2 ± 0.2 mg P/L
Soluble silicon	12 ± 1.5 mg Si/L
Sulphate	31 ± 1 mg SO ₄ ²⁻ /L
Dissolved organic carbon	18 ± 1 mg C/L
Inorganic carbon	106 ± 3 mg C/L

138

139 2.2.5. Adsorbent characterization

140 The types of iron oxide in the adsorbents were determined using Mössbauer spectroscopy. Transmission
 141 ⁵⁷Fe Mössbauer spectra were collected at different temperatures with conventional constant
 142 acceleration and sinusoidal velocity spectrometers using a ⁵⁷Co (Rh) source. Velocity calibration was
 143 carried out using an α-Fe foil. The Mössbauer spectra were fitted using the Mosswin 4.0 program.

144 For determining the surface area of the adsorbents, nitrogen adsorption and desorption cycles were
 145 carried out using Micromeritics TriStar 3000. The data from the nitrogen adsorption-desorption profiles
 146 were fitted with models included in the analysis software to obtain the pore area from Non Local
 147 Density Functional Theory (NLDFT) (Cracknell et al. 1995).

148 The elemental composition of the adsorbents was quantitatively measured by microwave digestion with
 149 67 % HNO₃. The elemental distribution on the adsorbent surface was monitored using scanning electron
 150 microscope coupled energy dispersive X-Ray (SEM-EDX). The imaging was done using a JEOL JSM-6480
 151 LV Scanning Electron Microscope. Elemental analysis was done at an acceleration voltage of 15 kV using
 152 Oxford Instruments x-act SDD Energy Dispersive X-ray Spectrometer. The composition of the surface

153 precipitates on the adsorbent was determined using Raman Spectroscopy (LabRam HR Raman
154 spectrometer).

155 Point of zero charge (PZC) of the adsorbents was determined by using the salt addition method
156 (Mahmood et al. 2011); 0.2 g of adsorbents (particle size < 0.35 mm) were added to aqueous solutions
157 of 0.1 M NaNO₃ with initial pH varying from 4 to 11. The NaNO₃ solution was bubbled with N₂ gas prior
158 to the adsorbent addition, and the experiment was conducted in a glovebox with N₂ atmosphere to
159 avoid effect of carbon dioxide on the pH. The adsorbents were allowed to mix for 48 hours and the final
160 pH was measured. The difference in initial and final pH was plotted against the initial pH values and the
161 PZC was defined by the pH where the difference in pH was zero. Table 3 shows the characteristics of the
162 adsorbents used.

163 **Table 3:** Adsorbent characteristics

Adsorbent	Type of adsorbent	Bulk density (g/cm ³)	Surface area (m ² /g)	Point of zero charge	Major constituents (wt%) ^a
GEH	Porous iron oxide	1.1	244	6.1	Fe – 51 %
FSP	Porous iron oxide	0.7	179	9.1	Fe – 47 %, Ca – 8 %
IEX ^b	Iron oxide impregnated in resin	0.7	58	6.6	Fe – 22 %, TOC – 25 %

164 ^a - Shows constituents comprising more than 5 wt % of adsorbent as measured after microwave digestion
165 of the samples

166 ^b – For the IEX the bulk density was measured in its default wet state, whereas for FSP and GEH the bulk
167 density was estimated in their dry forms.

168 2.2.6. Estimation of adsorption capacity

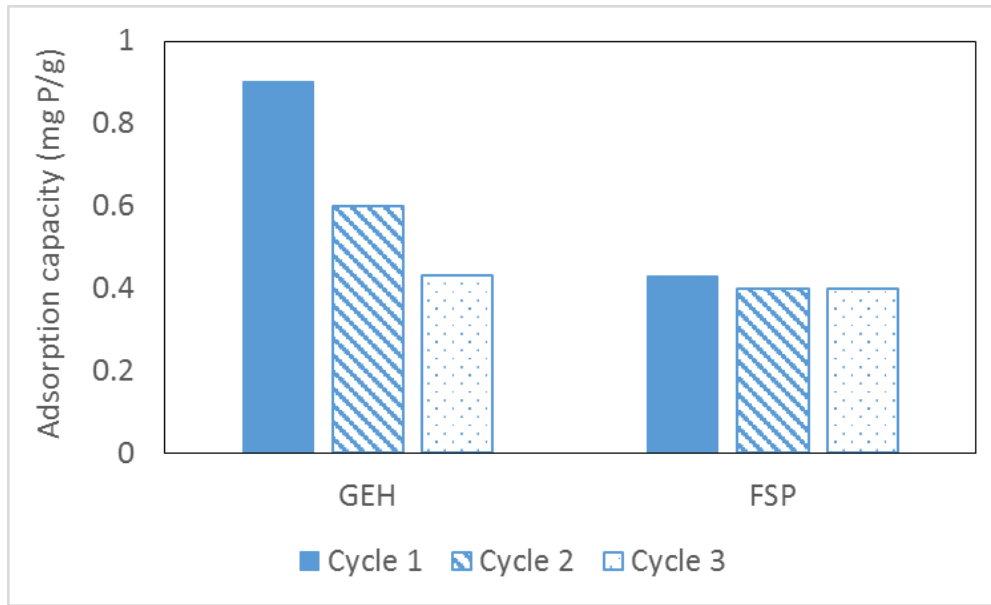
169 The phosphate adsorption capacity was calculated by evaluating breakthrough curves for the different
170 adsorbents. The breakthrough point was considered to be the point when the outlet phosphate
171 concentration from the columns reached 0.1 mg P/L. The detection limit for phosphate was 0.02 mg P/L.
172 The amount of phosphate adsorbed was calculated by plotting the concentration of phosphate removed
173 versus the volume of solution passed and estimating the area under the curve using trapezoidal rule
174 (Atkinson 1989).

175 3. Results and discussion

176

177 3.1. Optimization of phosphate adsorption and reusability by varying adsorbent 178 particle size and regeneration conditions

179 Fig 1 shows the phosphate adsorption capacities of GEH and FSP for 3 consecutive cycles using alkaline-
180 acid regeneration. The adsorption capacity was estimated from the breakthrough curves when the
181 phosphate concentration from the column outlet reached 0.1 mg P/L (fig S2 in supporting information
182 shows an example of such breakthrough curve).



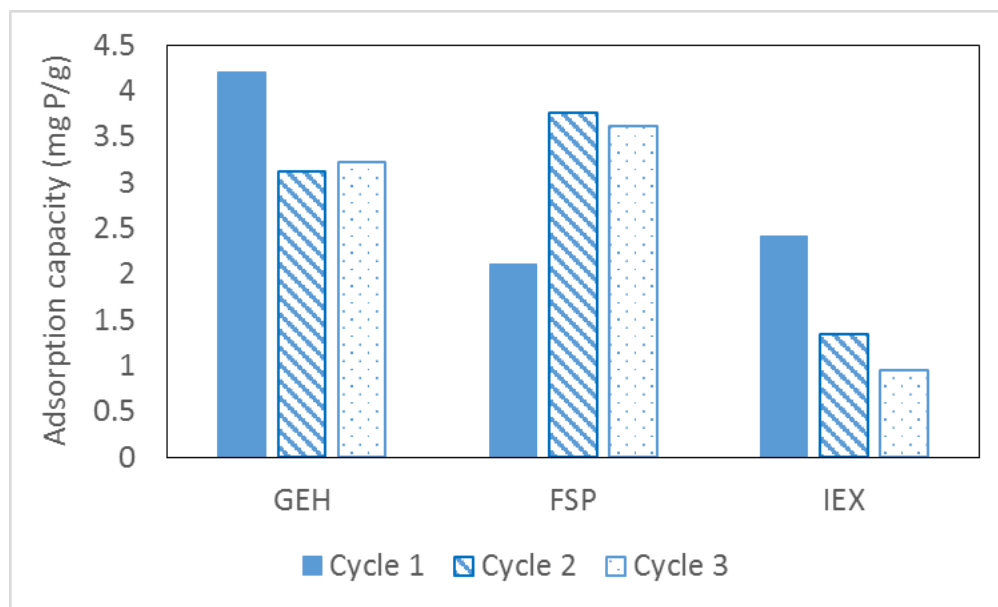
183

184 **Fig 1:** Adsorption capacities of 1 to 1.25 mm sized GEH and FSP for breakthrough at 0.1 mg P/L using
 185 alkaline-acid regeneration

186 Fig 1 shows that for the 1st cycle, the adsorption capacity of GEH and FSP at effluent concentration of 0.1
 187 mg P/L was around 0.9 and 0.4 mg P/g, respectively. A phosphate molecule has a diameter of 0.48 nm
 188 (Tawfik and Viola 2011). Assuming a monolayer coverage, these adsorption capacities correspond to an
 189 area of 3.1 m² for GEH and 1.4 m² for FSP. This implies only around 1 % of the overall surface area is
 190 covered in both these adsorbents. It must be noted that the values shown in fig 1 are not equilibrium
 191 adsorption capacities, but adsorption capacities estimated under the given EBCT of 5 minutes. The
 192 reason for such a low adsorption capacity corresponding to a very low area coverage fraction is likely
 193 due to the diffusion limitation in these porous adsorbents.

194 Moreover, the reusability of GEH was also affected significantly during these 3 cycles. The adsorption
 195 capacity for GEH dropped by 50 % by the 3rd cycle, whereas for FSP the adsorption capacity dropped by
 196 about 7 %.

197 To improve the reusability of the adsorbents, the regeneration order was reversed by first doing an acid
198 wash followed by alkaline desorption as suggested elsewhere (Kunaschk et al. 2015). To improve the
199 adsorption capacity of the adsorbents, GEH and FSP were grinded to a particle size of 0.25 to 0.325 mm,
200 which was similar to the particle size of the IEX adsorbent. Fig 2 shows the phosphate adsorption
201 capacities of GEH, FSP and IEX for 3 consecutive cycles using acid-alkaline regeneration.



202
203 **Fig 2:** Adsorption capacities of 0.25 to 0.325 mm sized GEH, FSP and IEX for breakthrough at 0.1 mg P/L
204 using acid-alkaline regeneration

205 Phosphate adsorption capacities for the 1st cycle of GEH and FSP were more than 4 times higher for the
206 0.25 to 0.325 mm sized particles as compared to the 1 to 1.25 mm sized particles. The specific surface
207 areas of the large (1 to 1.25 mm) and small (0.25 to 0.325 mm) sized adsorbents were similar (table S1).
208 GEH and FSP are porous adsorbents where the measured surface area is related to micropores (< 2 nm)
209 and mesopores (2 to 50 nm) (as per the NLDT method) (Cracknell et al. 1995). Thereby grinding them in
210 the mm range does not change their overall area. Porous adsorbents offer the advantage of high surface
211 area even in granular form, thereby allowing for easier handling and operation. However, the porous

212 nature of such adsorbents implies that the adsorption is limited by diffusion. Thereby, under non-
213 equilibrium conditions, decreasing their particle size increases the phosphate adsorption even though
214 their surface area stays the same (fig 1 and fig 2). This shows the need to consider the accessibility of the
215 pores properties while designing such adsorbents, especially for operations with short contact times.

216 The reusability of the GEH and FSP adsorbents were enhanced for the smaller particle sizes. The
217 decrease in adsorption capacity of GEH for the 2nd and 3rd cycles in figure 2 was less than the decrease
218 seen in fig 1. The adsorption capacity of FSP increased for the 2nd and 3rd cycles by a factor 2 as
219 compared to cycle 1. The adsorption capacity of IEX decreased by 50 % by the 3rd cycle.

220 Usually the reusability of adsorbents in lab scale experiments are demonstrated for 5 to 10 cycles
221 (Chitrakar et al. 2006, Kim et al. 2017, Wan et al. 2016). However, as can be seen from fig 1 and fig 2, we
222 see interesting trends in reusability of the adsorbents already by 3 cycles. This is also due to the complex
223 nature of the wastewater effluent as opposed to the cleaner solutions spiked with phosphate that are
224 often used to demonstrate successful reusability. Thus the focus of this study henceforth was to
225 understand the reason for these differing trends in reusability. By understanding what factors exactly
226 contribute to adsorbent reusability, the optimal procedures for regeneration can be designed. Even if 5
227 to 10 cycles of successful reuse can be demonstrated via the optimal regeneration methods and if it can
228 be shown that the adsorbent characteristics do not change over this period, then the adsorbent lifetime
229 can be extrapolated to longer reuse cycles.

230 3.2. Understanding phosphate adsorption and reusability by monitoring different 231 parameters

232 3.2.1. Effect of surface (porous) area

233 During the regeneration process the acid and alkaline treatment might cause the iron oxides to
234 solubilize and recrystallize. In such a case the physical as well as chemical properties of the iron oxide

235 can change, such as the change in surface area or the crystallinity/type of iron oxide. A change in surface
 236 area could lead to a loss of active sites which would thus affect the adsorbent reusability. Table 4 shows
 237 the overall change in adsorbent surface area along with the change in adsorption capacity for cycle 1
 238 and cycle 3 (raw data in table S1 in supporting information).

239 **Table 4:** Overall change in surface area (between 1st and 3rd cycles) for adsorbents regenerated using the
 240 alkaline-acid and acid-alkaline methods. The + and – signs imply increase or decrease.

Adsorbents	Regeneration using alkaline-acid method		Regeneration using acid-alkaline method	
	Change in surface area	Change in adsorption capacity	Change in surface area	Change in adsorption capacity
GEH	- 10 %	- 52 %	- 8 %	- 23 %
FSP	+ 25 %	- 7 %	+ 56 %	+ 71 %
IEX			+ 20 %	- 60 %

241
 242 In general, except for FSP regenerated using the acid-alkaline method, the change in surface area did
 243 not show a correlation with the change in adsorption capacity. This implies that the adsorbent
 244 reusability is also affected by other parameters.

245 3.2.2. Effect of the type of iron oxide in the adsorbent

246
 247 Phosphate adsorption happens on iron oxides via a ligand exchange mechanism with the surface
 248 hydroxyl groups (Parfitt et al. 1975). The change in the crystallinity/type of iron oxide during
 249 regeneration will lead to exposure of differing types and amount of surface hydroxyl groups which in

250 turn will affect the phosphate adsorption (Cornell and Schwertmann 2004). In an earlier study, a
 251 decrease in crystallinity of goethite decreased the adsorbent reusability within 2 cycles (Chitrakar et al.
 252 2006). The crystallinity of akaganeite stayed intact in the same study and the adsorbent could be reused
 253 successfully for 10 cycles. Apart from the regeneration chemicals, the binding of ions like silicate and
 254 organics from the wastewater can also influence the crystallinity of the adsorbents (Schwertmann et al.
 255 1984).

256 To measure if the type of iron oxide changes during the adsorbent usage, the adsorbents were
 257 measured with Mössbauer spectroscopy in their unused states and used state (after 3 adsorption
 258 cycles). During these cycles the adsorbents were regenerated using the acid-alkaline method which
 259 involved acid wash at pH 2.5 and alkaline desorption at pH 14. Table 5 shows the Mössbauer fitted
 260 parameters for the different adsorbents.

261 **Table 5:** The Mössbauer fitted parameters of different adsorbents in their unused and used
 262 states. Used state refers to the adsorbent after 3 adsorption cycles.

263

<i>Sample</i>	<i>T</i> (<i>K</i>)	<i>IS</i> (<i>mm·s⁻¹</i>)	<i>QS</i> (<i>mm·s⁻¹</i>)	<i>Hyperfine</i> <i>field (T)</i>	<i>Γ</i> (<i>mm·s⁻¹</i>)	<i>Phase</i>	<i>Spectral</i> <i>contribution (%)</i>
GEH	4.2	0.35	0.06	51.6	0.45	Fe ³⁺ (<i>Hematite</i>)	11
		0.35	-0.08	47.5*	0.44	Fe ³⁺ (<i>Ferrihydrite</i>)	89
GEH used	4.2	0.36	0.02	51.9	0.45	Fe ³⁺ (<i>Hematite</i>)	10
		0.35	-0.07	47.8*	0.45	Fe ³⁺ (<i>Ferrihydrite</i>)	90
FSP	4.2	0.33	-0.01	44.6*	0.53	Fe ³⁺ (<i>Ferrihydrite</i>)	100

FSP used	4.2	0.34	-0.01	48.0*	0.44	Fe ³⁺ (<i>Ferrihydrite</i>)	100
IEX	4.2	0.36	-0.15	50.6	0.39	Fe ³⁺ (<i>Goethite/Hematite</i>)	21
		0.36	0.11	52.8	0.45	Fe ³⁺ (<i>Hematite</i>)	7
		0.35	-0.10	46.3*	0.42	Fe ³⁺ (<i>Ferrihydrite</i>)	72
IEX used	4.2	0.36	-0.10	50.2	0.49	Fe ³⁺ (<i>Goethite/Hematite</i>)	31
		0.35	0.01	52.0	0.36	Fe ³⁺ (<i>Hematite</i>)	8
		0.35	-0.08	46.7*	0.45	Fe ³⁺ (<i>Ferrihydrite</i>)	61

264 Experimental uncertainties: Isomer shift: I.S. ± 0.01 mm s⁻¹; Quadrupole splitting:
265 Q.S. ± 0.01 mm s⁻¹; Line width: $\Gamma \pm 0.01$ mm s⁻¹; Hyperfine field: ± 0.1 T; Spectral
266 contribution: $\pm 3\%$. *Average magnetic field.

267 Based on the fitted parameters (Murad 1988), table 5 shows that ferrihydrite is present in all the
268 samples. GEH and IEX comprised of more than one type of iron oxide. The spectral contribution of the
269 different iron oxide phases shows the transformation between used and unused adsorbents.
270 For instance GEH does not undergo significant changes in its composition before and after adsorption. It
271 must be noted that GEH has previously been reported as akaganeite when analyzed using X-ray
272 diffraction (XRD)(Kolbe et al. 2011). But XRD detects only the crystalline part of the adsorbent whereas
273 Mossbauer spectroscopy can detect even the amorphous/nanocrystalline iron oxides making it a more
274 suitable method.
275 For FSP even though the iron oxide phase is ferrihydrite in both the used and unused samples, there is a
276 change in the hyperfine field. The unused FSP has a hyperfine field that is lower than the usual value for
277 ferrihydrite (Murad 1988, Murad; and Schwertmann 1980). It could be that the FSP transformed from an
278 adsorbent having a highly disordered to a more ordered ferrihydrite species. Usually the surface area is
279 higher for more amorphous iron oxides (Borggaard 2006). However in this case the used FSP, i.e. the
280 adsorbent having more crystalline ferrihydrite, showed a higher surface area (table S1). The surface area

281 of the used FSP increased by more than 56 % compared to the unused FSP. This could be the reason for
282 the increased adsorption capacity of the FSP after regeneration by the acid-alkaline method. But this
283 increase in surface area need not have been due to the transformation of iron oxide species but rather
284 due to the removal of surface precipitates as will be discussed later.

285 For IEX, the content of ferrihydrite decreased and the overall content of goethite/hematite increased by
286 10 %. This higher transformation of the iron oxide phase in the IEX compared to GEH and FSP could be
287 due to the nature of iron distribution in the adsorbent. FSP and GEH are bulk iron oxides, whereas IEX is
288 a resin impregnated with iron oxide nanoparticles. This means that the iron oxide particles in IEX have a
289 higher surface area to volume ratio. Thus the fraction of the total iron oxide that is accessible to
290 phosphate adsorption will be much higher in the IEX as compared to FSP and GEH. Hence, even if the
291 active sites in all the adsorbents underwent similar transformation during regeneration, the overall
292 change in iron oxide phase will be higher for the IEX. Goethite and hematite have lower phosphate
293 adsorption per unit area compared to ferrihydrite (Wang et al. 2013). So it is possible that this
294 transformation in the IEX contributes to decrease in its reusability. However the decrease in ferrihydrite
295 content is only 11 % whereas the decrease in adsorption capacity is about 60 %. Thus it can be
296 understood that transformation of the iron oxides alone is not affecting the reusability.

297 3.2.3. Effect of competing ions 298

299 To make the adsorbent reusable, it is necessary to regenerate the adsorbent properly, whereby the
300 adsorbate molecules are desorbed, and the active sites are replenished. The phosphate adsorption
301 experiments with 1 to 1.25 mm sized GEH and FSP granules were used to optimize the adsorption and
302 regeneration procedure. Apart from phosphate, different competing ions were monitored during
303 adsorption cycle 1. Based on these observations (shown in fig S3), selected ions were screened to be

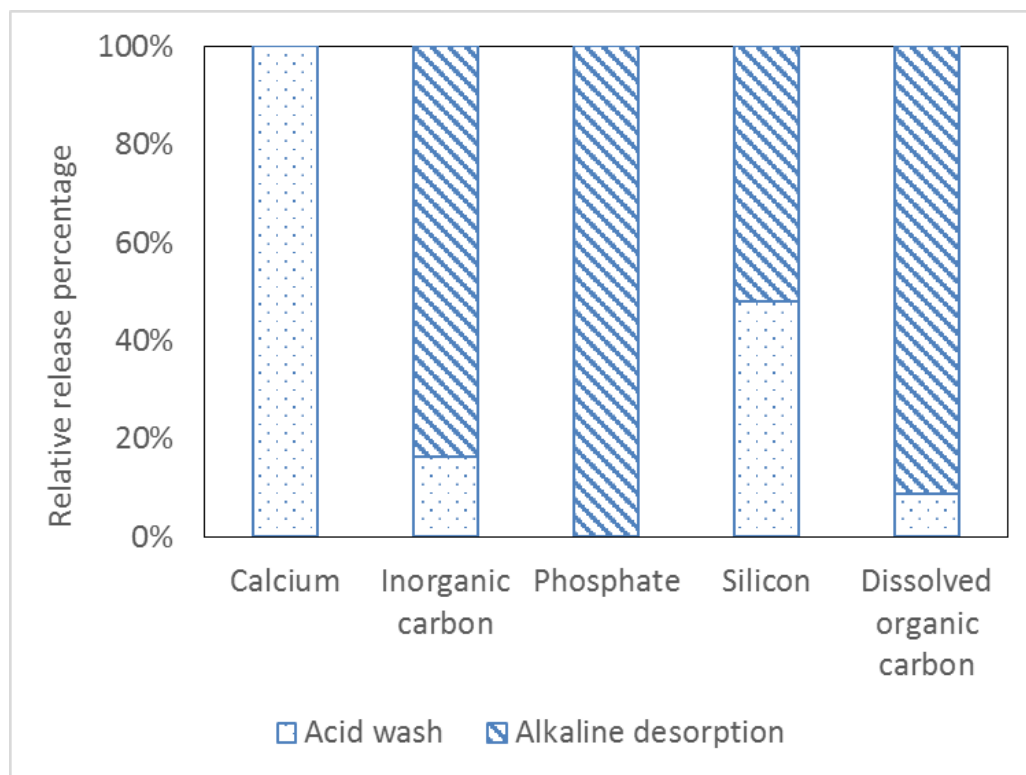
304 included in a mass balance while using adsorbents with particle size 0.25 to 0.325 mm. These included
305 calcium, organic carbon, inorganic carbon, silicon.

306 Values of the mass balance for the 0.25 to 0.325 mm sized adsorbents are shown in table S2 in the
307 supporting information. The mass balances could not be closed in several cases. For e.g. for GEH, the
308 silicon released during regeneration was always lower than the amount adsorbed, and for IEX, the
309 dissolved organic carbon released was always lower than amount adsorbed (shown in fig S4).

310 Calcium was monitored since it can form surface precipitates (Kunaschk et al. 2015). The release of
311 calcium from the different adsorbents regenerated using the acid-alkaline regeneration is shown in fig
312 S4. For GEH, the calcium release was less than 50 % in cycle 1. Thus the acid wash was switched from a
313 pH of 4 to pH of 2.5 for cycles 2 and 3, based on the earlier protocol (Kunaschk et al. 2015). This
314 improved the calcium release significantly amounting to 98 and 88 % for cycles 2 and 3. Iron
315 concentration was monitored in the acid wash to check if the adsorbent was leaching iron. Even using a
316 pH as low as 2.5, the amount of iron released per cycle for all the adsorbents was less than 0.01 % of the
317 adsorbent mass packed in the column. For FSP, the calcium release during cycle 1 and 2 was higher than
318 100 % since FSP by default consists of calcium (see table 3). For IEX, only around 20 % of calcium could
319 be released during cycles 2 and 3.

320 In this study, the alkaline desorption step was used to desorb ions like phosphate that bind with the
321 surface hydroxyl groups on the iron oxide. The acid wash step on the other hand was used to release the
322 surface precipitates. Thus the release of a competing ion in either the acid wash step or during alkaline
323 desorption gives information about its mechanism of binding on the adsorbent.

324 Fig 3 shows the average relative release percentages of different ions for FSP during acid wash and
325 alkaline desorption while using the acid-alkaline regeneration. The adsorbents GEH and IEX exhibited
326 similar release patterns for the different ions (fig S5).



328

329 **Fig 3:** Relative release percentage of different ions from FSP in acid wash and alkaline desorption (for
330 acid-alkaline regeneration)

331 From fig 3, it can be seen that calcium is released exclusively during acid wash whereas phosphate is
332 released exclusively via alkaline desorption. This was the case for all adsorbents (fig S5). This shows that
333 there is no formation of calcium phosphate precipitate and these ions bind via different mechanisms.

334 A majority of the inorganic carbon, which at this pH would represent (bi)carbonate ions, was released
335 during alkaline desorption. While it is possible that carbonate ions can sometimes adsorb via ligand
336 exchange on iron oxides (Chunming Su and Suarez 1997), it was expected that in this case carbonate
337 forms surface precipitates with calcium. But in these experiments the acid wash was done in an open
338 system. Therefore, if there were carbonate ions that were released during the acid wash, they would
339 have mostly escaped as carbon dioxide (Hey et al. 1994).

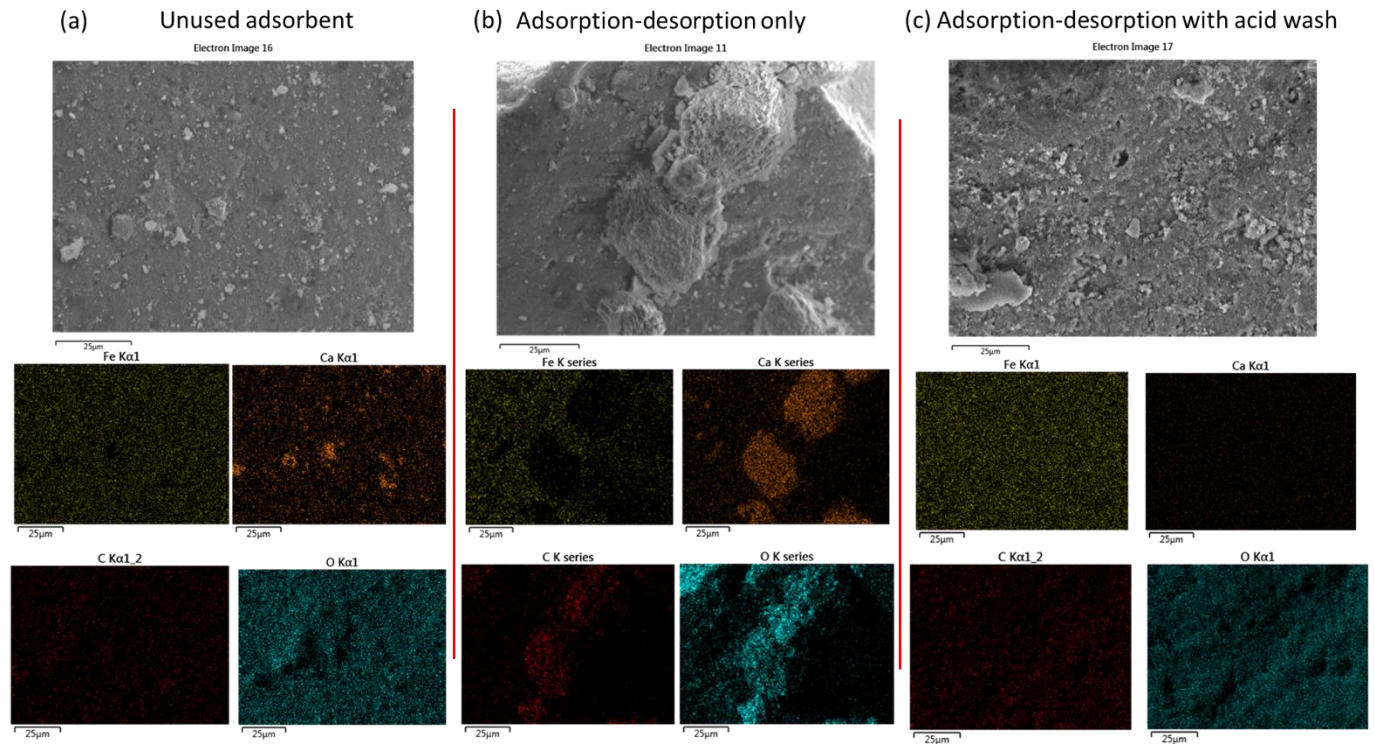
340 Soluble silicon was about equally released in acid wash as well as in alkaline desorption. Silicon present
341 as orthosilicates can bind as innersphere complexes that would be desorbed during alkaline desorption,
342 but could also form calcium silicate based precipitates that would dissolve in the acid wash (Lothenbach
343 and Nonat 2015, Sigg and Stumm 1981). Organic carbon was mostly released by alkaline desorption.
344 This is expected since organics like humics also bind to iron oxides via the ligand exchange with their
345 surface functional groups (Antelo et al. 2007, Ko et al. 2005).

346 These results shows that different ions bind on the adsorbent via different mechanisms and not all of
347 them are completely released. More regeneration cycles would show how this affects the adsorbent
348 reusability over time.

349 3.2.4. Effect of calcium based surface precipitation 350

351 The reason for using acid wash in the regeneration methods was based on the premise of removing
352 calcium based surface precipitates (Kunaschk et al. 2015). Fig 4 shows the SEM-EDX observations on the
353 unused FSP, FSP that had been used for 3 adsorption cycles using acid-alkaline regeneration, and FSP
354 that been used for 3 adsorption cycles but regenerated only using alkaline desorption. The color codes
355 for the elemental maps are stated in the figure caption.

356



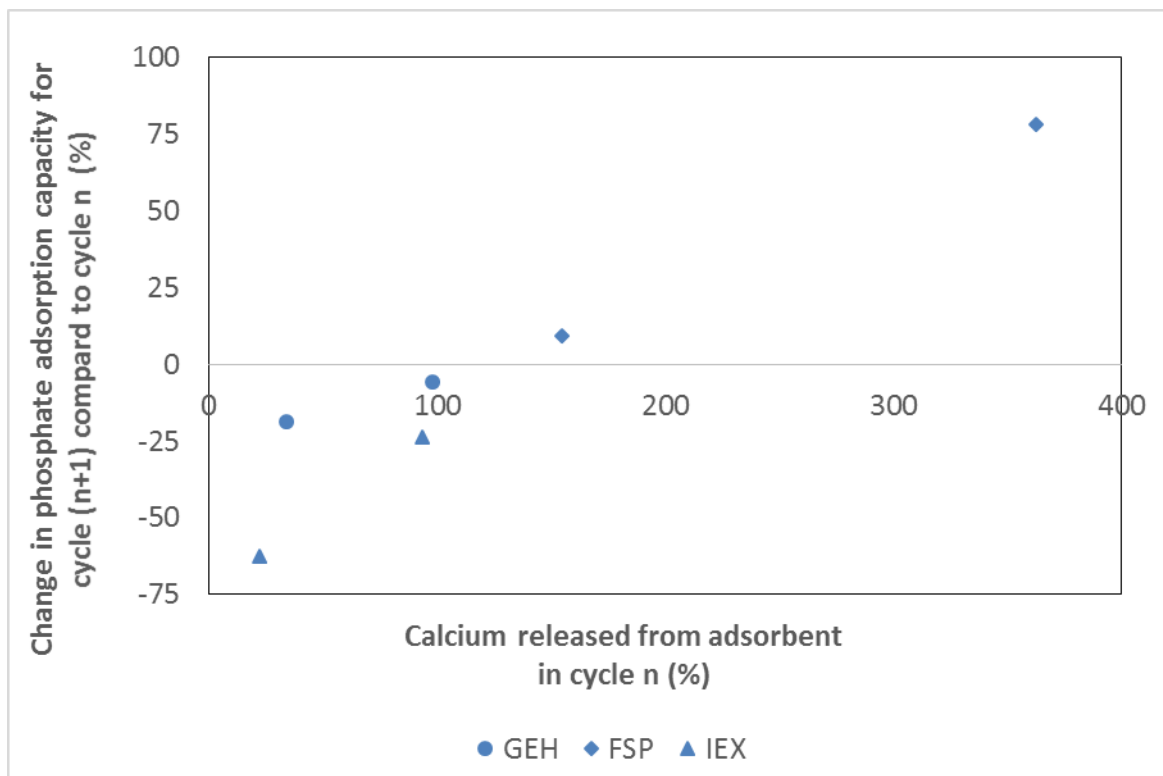
357

358 **Fig 4:** SEM-EDX observations of FSP adsorbent for (a) unused content (Ca content as per EDX = 5 wt %),
 359 (b) FSP regenerated without acid wash (Ca content = 15 wt %), (c) FSP regenerated with acid wash ash
 360 (Ca content = 0 wt %). Scalebar represent 25 μm. Color code for elemental maps- Yellow = Iron, Orange
 361 = Calcium, Red = Carbon, Blue = Oxygen.

362 It can be seen from fig 4 (a), that unused FSP has calcium by default. But the elemental map of calcium
 363 and carbon do not overlap implying there is no observable calcium carbonate. Fig 4 (b) shows the FSP
 364 that was regenerated only with alkaline desorption and no acid wash. There are large areas in the
 365 elemental distribution where calcium, carbon and oxygen overlap. This implies the presence of calcium
 366 carbonate. The observable calcium carbonate particles are about 25 μm in size. Fig 4 (c) shows that the
 367 acid washed FSP (using acid-alkaline regeneration) has no calcium left and thus the surface precipitates
 368 are removed via acid wash. This was confirmed by Raman spectroscopy where the FSP regenerated
 369 without acid wash showed Raman shift characteristics of calcium carbonate (shown in fig S6).

370 This result is in line with the observations in fig 3 and fig S5 that the calcium was released exclusively via
371 the acid wash and hence must be present in the form of surface precipitates. While calcium carbonate
372 was the only precipitate that was observable, some silicon was also released during the acid wash (fig 3),
373 indicating the possibility of calcium silicate precipitates. However, the molar ratio of inorganic carbon to
374 silicon present in the wastewater was more than 20 (as seen from table 2), and the solubility product for
375 calcium carbonate is lower than calcium silicate (Benjamin 2010, Greenberg et al. 1960). Thus calcium
376 carbonates are likely the dominant precipitates formed on the adsorbent surface.

377 To test for the effect of calcium based surface precipitates on the adsorbent reusability, the extent of
378 calcium release from the adsorbents was correlated with the adsorption capacities. Fig 5 shows the
379 change in phosphate adsorption capacity for a given cycle compared to the calcium released from the
380 previous cycle. n+1 denotes the current cycle and n denotes the previous cycle.



381

382 **Fig 5:** Change in phosphate adsorption capacity for a given cycle compared to the calcium release in the
383 previous cycle (using acid-alkaline regeneration). $n+1$ is used to denote the current cycle and n denotes
384 the previous cycle. $n = 1,2$. A negative change in the phosphate adsorption capacity implies the
385 adsorbent reusability decreases whereas a positive change implies the reusability is enhanced.

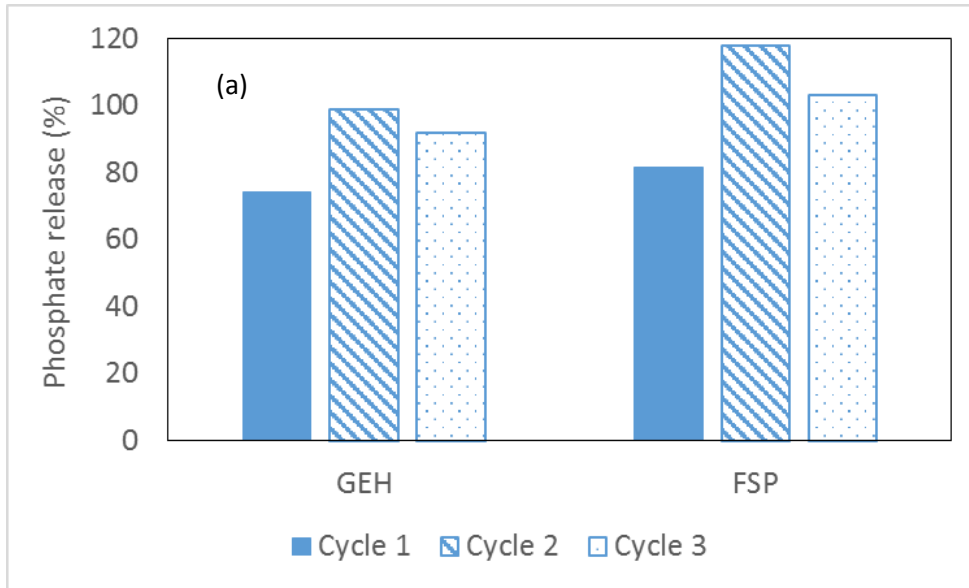
386 Fig 5 includes data points from all the adsorbents regenerated using the acid-alkaline method. The data
387 points showing more than 100 % calcium release are from FSP, since it contained calcium by default. The
388 general trend observed is that the change in phosphate adsorption capacity is negative, i.e. the
389 adsorbent reusability decreases, if not all the calcium from the adsorbent is released. This agrees with
390 the reasoning that the calcium carbonate precipitates affect the adsorbent reusability and needs to be
391 removed via an acid wash.

392 3.3. Mechanism of decrease in adsorbent reusability via surface precipitation 393

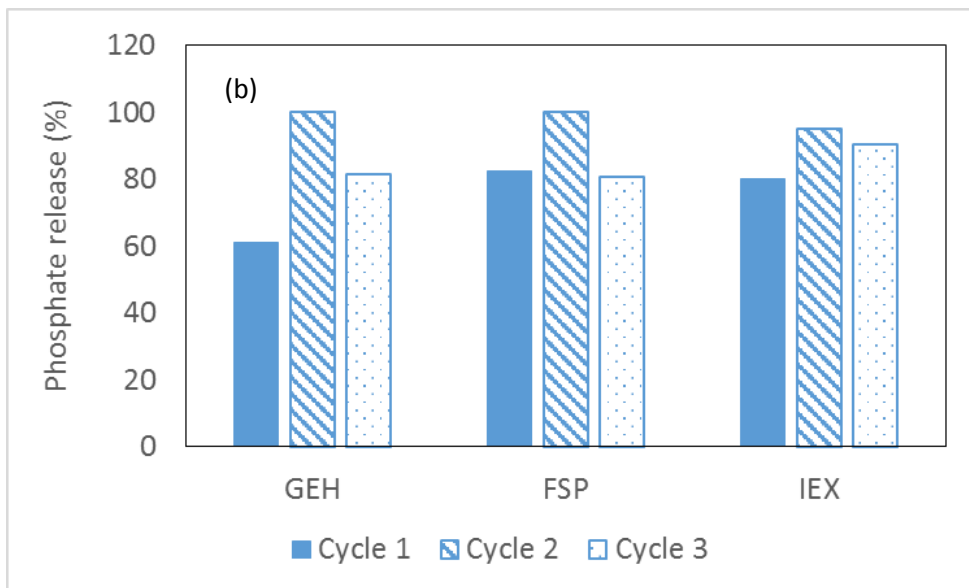
394 3.3.1. Hypothesis based on desorption of phosphate 395

396 The above results show the need for an acid wash step to remove the calcium based surface
397 precipitates. As per the earlier study, having an acid wash step before alkaline desorption resulted in
398 better adsorbent reusability than the other way around (Kunaschk et al. 2015). The explanation
399 provided in that study was that adsorbed phosphate was blocked by surface precipitates. Thus the
400 surface precipitates need to be first released before the phosphate can be released via alkaline
401 desorption (a depiction of this hypothesis is shown in fig S7). This hypothesis was tested in our study by
402 reversing the order of regeneration and checking the extent of phosphate released during regeneration.
403 If the hypothesis is correct, then having an acid wash step after alkaline desorption should lead to a
404 lower desorption of phosphate. Fig 6 (a) and (b) show phosphate released during alkaline desorption for
405 the adsorbents used in the experiments corresponding to fig 1 and fig 2, respectively. The release
406 percentage was calculated by measuring the amount desorbed in relation to the amount adsorbed.

407



408



409

410 **Fig 6:** Percentage of phosphate released during alkaline desorption step using (a) alkaline-acid
411 regeneration (b) acid-alkaline regeneration.

412 The phosphate release from all adsorbents mostly varied between 80 to 100 % using both regeneration
413 methods. From fig 6 (a) it can be seen that FSP released more than 100 % phosphate for the 2nd cycle.

414 This could have come from the phosphate that was not released during the 1st cycle. Comparing fig 6 (a)

415 and 6 (b), there was no significant difference in the phosphate released by the two different
416 regeneration methods. Thus, we conclude the differences in reusability as seen in fig 1 and fig 2 are
417 apparently not due to blockage of adsorbed phosphate molecules as suggested in the earlier hypothesis.
418 This implies that the reason for differences in reusability for GEH and FSP between the two regeneration
419 methods (as seen in fig 1 and fig 2) was due to the differences in the acid wash conditions. In the
420 alkaline-acid regeneration, a pH of 4 was used for the acid wash step. This was to make sure iron
421 dissolution from the iron oxides does not happen. In the acid-alkaline regeneration, we tried to improve
422 the reusability by having stronger acid wash conditions. This was done by first having longer exposure
423 time with pH 4. However, the calcium release from GEH was still less than 50 % (table S2 and fig S4).
424 Thus a stronger acidic pH of 2.5 was used as suggested previously (Kunaschk et al. 2015). We noticed
425 that no significant iron was leached from the acid wash implying that the acid was consumed primarily
426 for breaking the surface precipitates. Thus the enhanced reusability was due to the release of surface
427 precipitates. But apparently the surface precipitates do not hinder reusability by just blocking
428 the adsorbed phosphate. This implies that there could be some additional mechanism by which surface
429 precipitation affects reusability.

430 3.3.2. Possible role of calcium adsorption

431

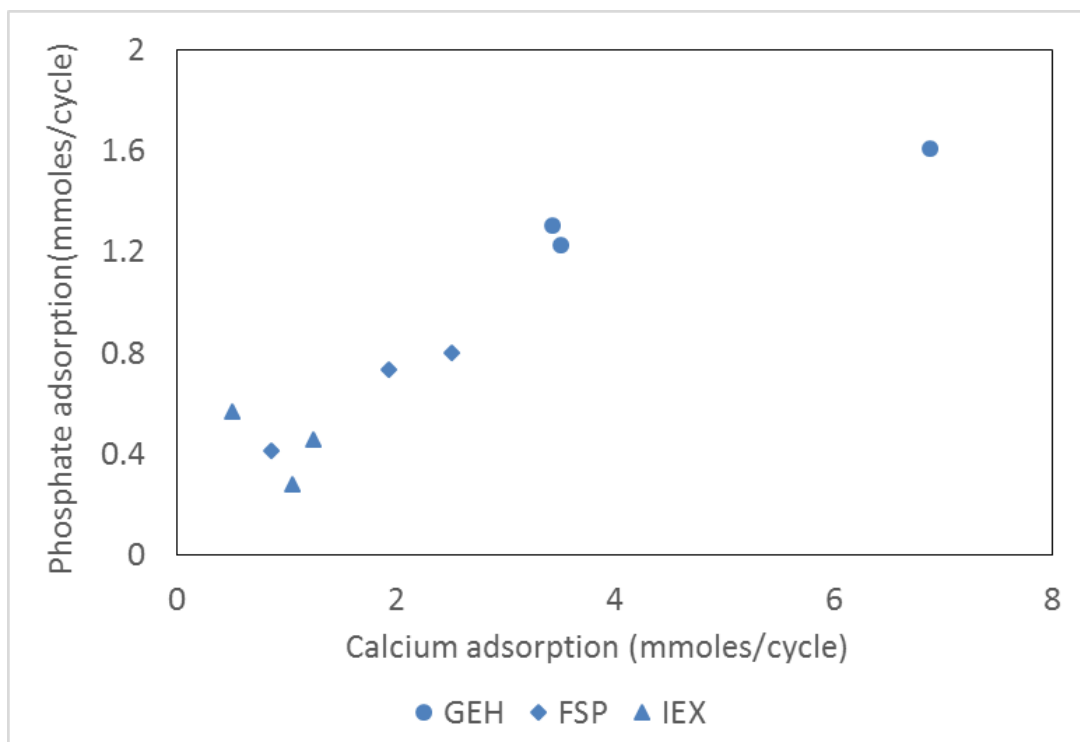
432 It could be that the calcium based surface precipitates block the active sites for phosphate on the
433 adsorbent. However, as seen from fig 3 and fig S5, calcium binds on the adsorbent via a different
434 mechanism to phosphate and hence should not directly block the active sites. In the case of FSP, the
435 adsorbent already contains calcium in its unused state. If this calcium was present as precipitates
436 blocking the adsorbent pores or covering the iron oxide, the removal of this calcium during washing
437 would expose active sites on the adsorbent that were previously inaccessible. This could be a reason for

438 the increase in the surface area and the adsorption capacity of FSP for the 2nd and 3rd cycle when using
439 acid-alkaline regeneration (fig 2).

440 Another possible way that calcium carbonate precipitates can affect the adsorbent reusability is by
441 changing the point of zero charge (PZC) of the adsorbent and affecting the adsorption of calcium on
442 them. Also, calcium ions are known to bind to iron oxide surfaces and enhance phosphate adsorption by
443 making the surface electropositive (Antelo et al. 2015, Han et al. 2017, Rietra et al. 2001). A study
444 testing GEH for adsorption of phosphonate, which binds to iron oxides in a similar mechanism as
445 phosphate, reported that phosphonate adsorption at equilibrium doubled in a solution having a Ca:P
446 molar ratio of 2 as compared to a solution without any calcium (Boels et al. 2012). This implies calcium
447 adsorption onto GEH could result in a favorable equilibrium shift for phosphate adsorption as well.

448 Fig 7 shows the calcium and phosphate adsorption for all the adsorbents during all adsorption cycles for
449 acid-alkaline regeneration. This includes only the calcium that was adsorbed during the adsorption
450 process and does not consider the calcium that is by default in the FSP adsorbent. A positive correlation
451 was observed between overall adsorption of calcium and phosphate ions.

452



453

454 **Fig 7:** Correlation of Ca vs P adsorption (including all cycles for all adsorbents using acid-alkaline
455 regeneration)

456 Calcium likely first physisorbs on the adsorbent surface before it forms calcium carbonate precipitates.
457 Physisorption of calcium would enhance phosphate adsorption by making the surface electropositive
458 (Antelo et al. 2015). Studies show that significant calcium binding happens only at a pH higher than the
459 PZC of the adsorbent (Antelo et al. 2015, Rietra et al. 2001). At pH higher than PZC, the adsorbent
460 surface is electronegative which will enhance calcium binding. Thus if an adsorbent has lower PZC than
461 the pH of wastewater effluent, more calcium would bind to the adsorbent, which in turn would enhance
462 the P adsorption. The pH of the wastewater effluent was 7.9 and the PZC for GEH and FSP was 6.1 and
463 9.1, respectively. This could be the reason why more calcium binds to GEH in cycle 1 compared to FSP
464 (table S2 and fig S3). Hence GEH shows a higher phosphate adsorption capacity for cycle 1 than FSP.

465 However, the PZC on the adsorbent could shift upon the binding of calcium. Calcium carbonates have
466 often shown PZC that are higher than 9 (Al Mahrouqi et al. 2017). The formation of calcium carbonate
467 precipitates could thus increase the PZC of the adsorbent. This would usually be more favourable for
468 phosphate adsorption since the adsorbent surface is more electropositive at a given pH. However, a
469 higher PZC would mean less calcium adsorption, which in turn would imply less phosphate adsorption.

470 PZC measurements (fig S8) supported the above speculation. FSP with calcium carbonate had a higher
471 PZC (PZC = 9.8), than the unused FSP which had some calcium (PZC = 9) and the acid-washed FSP which
472 had no calcium (PZC = 7.5). These PZC's were determined using the salt addition method which depends
473 on the pH measurements (Mahmood et al. 2011). This commonly used method can however have a
474 shortcoming when measuring PZC of porous materials because impurities/unwashed ions (like
475 hydroxide ions) in the pores can affect the measurement. Thus to prove/disprove this hypothesis, more
476 accurate methods like zeta potential measurements should be used to determine surface charge.

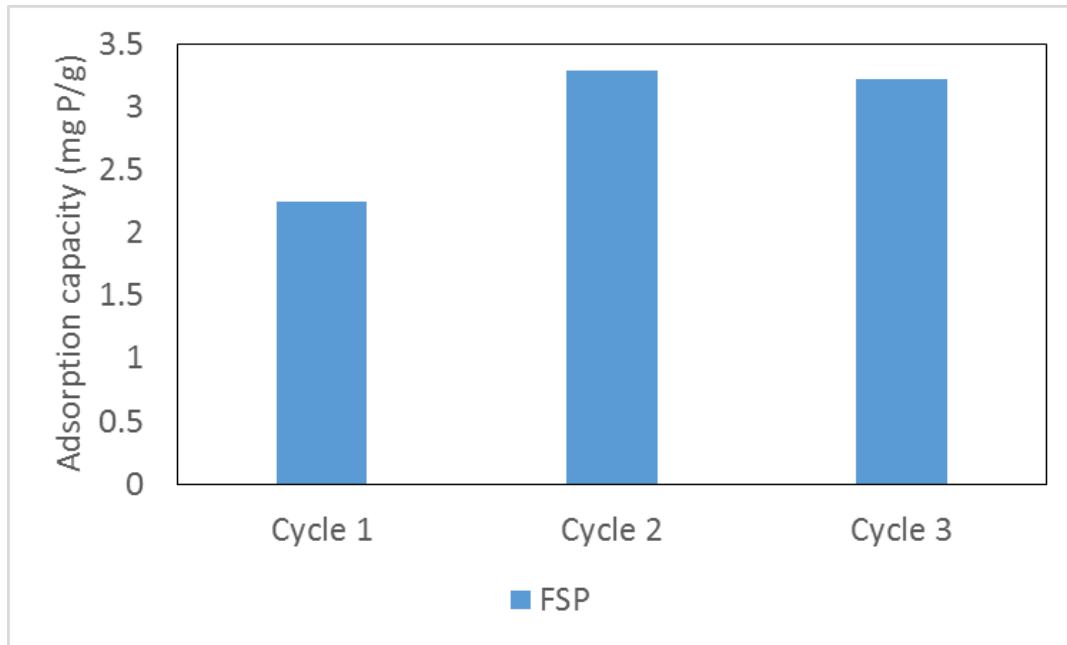
477 For IEX, the correlation with calcium is not as strong. In the case of IEX, the decrease in reusability could
478 thereby be due to multiple reasons like transformation of iron oxide phase and incomplete release of
479 adsorbed organics. The incomplete release of organics from IEX could be related to the nature of
480 regeneration. Hybrid ion exchange resins have been shown to remove anions via a combination of
481 mechanisms involving ligand exchange on the iron oxide as well as coulombic interaction on the
482 functional groups of the resin backbone (Sengupta and Pandit 2011). That study used a combination of
483 sodium chloride (NaCl) and NaOH solutions for regeneration and reported ten successful regeneration
484 cycles. However, the adsorption was studied for solutions containing only phosphate and sulphate ions
485 unlike the wastewater effluent which also contains organics. Organics like humic acids also bind to
486 hybrid ion exchange resins via the functional groups on the resin backbone as well as the iron oxides
487 impregnated within them (Shuang et al. 2013). Hence regeneration with only NaOH might not release
488 the organics bound on the functional groups of the resin. Although such organics might not compete

489 with the active sites for phosphate directly, the binding of humics might confer a negative charge to the
490 adsorbent (Antelo et al. 2007). This would be similar to a Donnan ion exclusion effect which would
491 hinder the transport of anions into the resin and hence reduce phosphate adsorption in subsequent
492 cycles (Cumbal and SenGupta 2005).

493 3.4. Adsorbent regeneration from a practical point of view

494
495 In regeneration methods involving acid wash, the pH in the adsorbent column was neutralized after the
496 regeneration process. In some of these cases, when the alkaline desorption was the last step, more than
497 1000 bed volumes of distilled water were required to neutralize the column. To reduce the bed volume
498 needed to neutralize the pH in these cases, the distilled water was spiked with HCl solution of pH 4.

499 In practice, a regeneration method producing minimal amount of waste and consuming the least
500 chemicals should be employed. Moreover we also wanted to check if an acid wash was necessary prior
501 to every adsorption cycle. In the current experiment, after alkaline desorption, the column was rinsed
502 with 50 bed volumes of distilled water but the pH in the pores was still not neutralized. Subsequent
503 adsorption runs were performed as such. Fig 8 shows the reusability of FSP when this regeneration
504 strategy was used.



505

506 **Fig 8:** Adsorption capacity at effluent concentration of 0.1 mg P/L for FSP regenerated using only alkaline
 507 desorption. Adsorbent particle size was 0.25 to 0.325 mm.

508 Fig 8 shows that the phosphate adsorption capacity increased for cycle 2 and cycle 3. From mass
 509 balances (table S3), it was seen that amount of calcium bound to the adsorbent increased by a factor of
 510 about 7 times for cycles 2 and 3 compared to cycle 1. When comparing the pH profile from the column
 511 effluent with the calcium removal by the adsorbent, it was seen that the increase in calcium uptake
 512 coincided with higher effluent pH (fig S9).

513 The increase in calcium binding is likely because the pH inside the pores of the regenerated adsorbent is
 514 higher than the PZC. Thus a high amount of calcium could bind to the adsorbent in such cases, which
 515 could also enhance phosphate adsorption. During such a regeneration method there is also a possibility
 516 of calcium phosphate precipitation. This would happen in the initial bed volumes of the adsorption run
 517 where the pH is high. Results from mass balance calculations (table S3) show that the average
 518 phosphate release via alkaline desorption during this regeneration method is about 1.5 times lower than
 519 regeneration methods 1 and 2. This implies that some phosphate is bound as surface precipitates and

520 hence this would be released only via acid wash. Thus an acid wash would probably be needed after
 521 some adsorption cycles.

522 Based on our observations, we can envision 3 different strategies for adsorbent regeneration as listed in
 523 table 6.

524 **Table 6:** Different regeneration strategies with their advantages and disadvantages

Regeneration method	Advantages	Disadvantages
Alkaline desorption with acid wash during every cycle	<ul style="list-style-type: none"> • Adsorption capacity is retained for each cycle • No buildup of surface precipitates after every cycle 	<ul style="list-style-type: none"> • Neutralization of adsorbent bed required after every cycle • More chemical consumption during regeneration than other methods
Alkaline desorption each cycle, with intermittent acid wash in between some cycles	<ul style="list-style-type: none"> • Neutralization of adsorbent bed is not required after every cycle • Adsorption capacity will be retained for some cycles before adsorbent needs acid wash 	<ul style="list-style-type: none"> • Calcium phosphate precipitation occurs • Part of phosphate will be release in acid wash
Alkaline desorption with no acid wash at all	<ul style="list-style-type: none"> • No acid consumption 	<ul style="list-style-type: none"> • This is a viable option only if calcium

	<ul style="list-style-type: none"> Least chemical consumption compared to other regeneration methods 	<ul style="list-style-type: none"> carbonate precipitation does not happen Phosphate adsorption capacity will be lower in the absence of calcium adsorption
--	---	---

525

526 In our study, we have used fresh acid and alkaline solutions for every regeneration step. In practice, the
527 regenerate solutions would need to be reused to make the process more cost effective. We noticed that
528 more than 250 bed volumes of acid wash solution of pH 2.5 were consumed while regenerating the FSP
529 adsorbent. This would thus be attributed to waste generated during the regeneration process unless the
530 solution can be reused over many cycles by only replenishing the acid consumed. One way to overcome
531 this problem is to prevent surface precipitation in the first place and hence prevent an acid wash step,
532 which is the 3rd type of regeneration strategy we highlight in table 6. To prevent/minimize surface
533 precipitation, the mechanism of calcium binding needs to be understood better. Understanding this
534 mechanism could help modify adsorbent properties such that calcium binding could be moderated. This
535 can be used to enhance phosphate adsorption due to co-adsorption of calcium but minimize surface
536 precipitation to lower acid consumption. For e.g. changing the adsorbent surface charge could be a
537 strategy to moderate calcium binding.

538 Moreover, we have only shown 3 adsorption-regeneration cycles in our study. The adsorbent would
539 need to last several adsorption cycles in practice. Hence future studies should also test the reusability
540 over more adsorption-regeneration cycles.

541 4. Conclusion

542

543 This research has monitored various aspects that could affect the phosphate adsorption and reusability
544 of adsorbents in a wastewater effluent.

- 545 • Despite having similar surface area, smaller adsorbent particles (0.25 to 0.325 mm) exhibited
546 more than 4 times higher phosphate adsorption capacities than larger adsorbent particles (1 to
547 1.25 mm). This points at the importance of diffusion in porous adsorbents.
- 548 • In most cases only minor changes were noticed for the adsorbents in the type of iron oxide and
549 surface area after 3 cycles of reuse. These changes were not significant to explain changes in
550 reusability of the adsorbent.
- 551 • Reversing the order of acid wash and alkaline desorption steps during regeneration did not
552 affect the desorption of phosphate during the 3 cycles.
- 553 • Calcium enhanced phosphate adsorption but also formed calcium carbonate based precipitates
554 on the adsorbent which need to be removed to maintain reusability.
- 555 • Future studies should focus on understanding the mechanism of calcium binding and monitoring
556 the reusability for more cycles.

557 5. Acknowledgements

558 This work was performed in the TTIW-cooperation framework of Wetsus, European Centre Of Excellence
559 For Sustainable Water Technology (www.wetusus.nl). Wetusus is funded by the Dutch Ministry of Economic
560 Affairs, the European Union Regional Development Fund, the Province of Friesland, the City of
561 Leeuwarden and the EZ/Kompas program of the “Samenwerkingsverband Noord-Nederland”. We thank
562 the participants of the research theme “Phosphate Recovery” for their financial support and helpful
563 discussions.

6. References

- 564
565
- 566 Al Mahrouqi, D., Vinogradov, J. and Jackson, M.D. (2017) Zeta potential of artificial and natural calcite in
567 aqueous solution. *Advances in Colloid and Interface Science* 240, 60-76.
- 568 Antelo, J., Arce, F., Avena, M., Fiol, S., López, R. and Macías, F. (2007) Adsorption of a soil humic acid at
569 the surface of goethite and its competitive interaction with phosphate. *Geoderma* 138(1), 12-19.
- 570 Antelo, J., Arce, F. and Fiol, S. (2015) Arsenate and phosphate adsorption on ferrihydrite nanoparticles.
571 Synergetic interaction with calcium ions. *Chemical Geology* 410, 53-62.
- 572 Atkinson, K. (1989) *An Introduction to Numerical Analysis*, Wiley.
- 573 Benjamin, M.M. (2010) *Water Chemistry*, Waveland Press, Incorporated.
- 574 Blaney, L.M., Cinar, S. and SenGupta, A.K. (2007) Hybrid anion exchanger for trace phosphate removal
575 from water and wastewater. *Water Research* 41(7), 1603-1613.
- 576 Boels, L., Keesman, K.J. and Witkamp, G.J. (2012) Adsorption of phosphonate antiscalant from reverse
577 osmosis membrane concentrate onto granular ferric hydroxide. *Environ Sci Technol* 46(17), 9638-9645.
- 578 Borggaard, O. (2006) Influence of iron oxides on the surface area of soil.
- 579 Cabrera, F., de Arambarri, P., Madrid, L. and Toga, C.G. (1981) Desorption of phosphate from iron oxides
580 in relation to equilibrium pH and porosity. *Geoderma* 26(3), 203-216.
- 581 Chitrakar, R., Tezuka, S., Sonoda, A., Sakane, K., Ooi, K. and Hirotsu, T. (2006) Phosphate adsorption on
582 synthetic goethite and akaganeite. *Journal of Colloid and Interface Science* 298(2), 602-608.
- 583 Chunming Su and Suarez, D.L. (1997) In situ infrared speciation of adsorbed carbonate on aluminum and
584 iron oxides. *Clays and Clay Minerals* 45(6), 814-825.
- 585 Cordell, D., Drangert, J.-O. and White, S. (2009) The story of phosphorus: Global food security and food
586 for thought. *Global Environmental Change* 19(2), 292-305.
- 587 Cornell, R.M. and Schwertmann, U. (2004) *The Iron Oxides*, pp. 253-296, Wiley-VCH Verlag GmbH & Co.
588 KGaA.

589 Cracknell, R.F., Gubbins, K.E., Maddox, M. and Nicholson, D. (1995) Modeling Fluid Behavior in Well-
590 Characterized Porous Materials. *Accounts of Chemical Research* 28(7), 281-288.

591 Cumbal, L. and SenGupta, A.K. (2005) Arsenic Removal Using Polymer-Supported Hydrated Iron(III)
592 Oxide Nanoparticles: Role of Donnan Membrane Effect. *Environmental Science & Technology* 39(17),
593 6508-6515.

594 Greenberg, S.A., Chang, T.N. and Anderson, E. (1960) INVESTIGATION OF COLLOIDAL HYDRATED
595 CALCIUM SILICATES. I. SOLUBILITY PRODUCTS. *The Journal of Physical Chemistry* 64(9), 1151-1157.

596 Han, C., Lalley, J., Iyanna, N. and Nadagouda, M.N. (2017) Removal of phosphate using calcium and
597 magnesium-modified iron-based adsorbents. *Materials Chemistry and Physics* 198, 115-124.

598 Hey, M.J., Hilton, A.M. and Bee, R.D. (1994) The formation and growth of carbon dioxide gas bubbles
599 from supersaturated aqueous solutions. *Food Chemistry* 51(4), 349-357.

600 Kalaitzidou, K., Mitrakas, M., Raptopoulou, C., Tolkou, A., Palasantza, P.-A. and Zouboulis, A. (2016) Pilot-
601 Scale Phosphate Recovery from Secondary Wastewater Effluents.

602 Kim, M., Kim, H. and Byeon, S.H. (2017) Layered Yttrium Hydroxide $l\text{-Y}(\text{OH})_3$ Luminescent Adsorbent for
603 Detection and Recovery of Phosphate from Water over a Wide pH Range. *ACS Appl Mater Interfaces*
604 9(46), 40461-40470.

605 Ko, I., Kim, J.-Y. and Kim, K.-W. (2005) Adsorption properties of soil humic and fulvic acids by hematite.
606 *Chemical Speciation & Bioavailability* 17(2), 41-48.

607 Kolbe, F., Weiss, H., Morgenstern, P., Wennrich, R., Lorenz, W., Schurk, K., Stanjek, H. and Daus, B.
608 (2011) Sorption of aqueous antimony and arsenic species onto akaganeite. *Journal of Colloid and*
609 *Interface Science* 357(2), 460-465.

610 Kunaschk, M., Schmalz, V., Dietrich, N., Dittmar, T. and Worch, E. (2015) Novel regeneration method for
611 phosphate loaded granular ferric (hydr)oxide – A contribution to phosphorus recycling. *Water Research*
612 71, 219-226.

613 L. Correll, D. (1998) The Role of Phosphorus in the Eutrophication of Receiving Waters: A Review.

614 Li, M., Liu, J., Xu, Y. and Qian, G. (2016) Phosphate adsorption on metal oxides and metal hydroxides: A
615 comparative review. *Environmental Reviews* 24(3), 319-332.

616 Loganathan, P., Vigneswaran, S., Kandasamy, J. and Bolan, N.S. (2014) Removal and Recovery of
617 Phosphate From Water Using Sorption. *Critical Reviews in Environmental Science and Technology* 44(8),
618 847-907.

619 Lothenbach, B. and Nonat, A. (2015) Calcium silicate hydrates: Solid and liquid phase composition.
620 *Cement and Concrete Research* 78, 57-70.

621 Mahmood, T., Saddique, M.T., Naeem, A., Westerhoff, P., Mustafa, S. and Alum, A. (2011) Comparison
622 of Different Methods for the Point of Zero Charge Determination of NiO. *Industrial & Engineering*
623 *Chemistry Research* 50(17), 10017-10023.

624 Murad, E. (1988) Iron in Soils and Clay Minerals. Stucki, J.W., Goodman, B.A. and Schwertmann, U. (eds),
625 pp. 309-350, Springer Netherlands, Dordrecht.

626 Murad, E. and Schwertmann, U. (1980) The Moessbauer spectrum of ferrihydrite and its relations to
627 those of other iron oxides. *American Mineralogist* 65(9-10), 1044-1049.

628 Parfitt, R.L., Atkinson, R.J. and Smart, R.S.C. (1975) The Mechanism of Phosphate Fixation by Iron Oxides
629 1. *Soil Science Society of America Journal* 39(5), 837-841.

630 Rietra, R.P.J.J., Hiemstra, T. and van Riemsdijk, W.H. (2001) Interaction between Calcium and Phosphate
631 Adsorption on Goethite. *Environmental Science & Technology* 35(16), 3369-3374.

632 Schwertmann, U., Carlson, L. and Fechter, H. (1984) Iron oxide formation in artificial ground waters.
633 *Schweizerische Zeitschrift für Hydrologie* 46(2), 185-191.

634 Sengupta, S. and Pandit, A. (2011) Selective removal of phosphorus from wastewater combined with its
635 recovery as a solid-phase fertilizer. *Water Research* 45(11), 3318-3330.

636 Shuang, C., Wang, M., Zhou, Q., Zhou, W. and Li, A. (2013) Enhanced adsorption and antifouling
637 performance of anion-exchange resin by the effect of incorporated Fe₃O₄ for removing humic acid.
638 Water Research 47(16), 6406-6414.

639 Sigg, L. and Stumm, W. (1981) The interaction of anions and weak acids with the hydrous goethite (α -
640 FeOOH) surface. Colloids and Surfaces 2(2), 101-117.

641 Tawfik, D.S. and Viola, R.E. (2011) Arsenate Replacing Phosphate: Alternative Life Chemistries and Ion
642 Promiscuity. Biochemistry 50(7), 1128-1134.

643 Wan, J., Tao, T., Zhang, Y., Liang, X., Zhou, A. and Zhu, C. (2016) Phosphate adsorption on novel hydrogel
644 beads with interpenetrating network (IPN) structure in aqueous solutions: kinetics, isotherms and
645 regeneration. RSC Advances 6(28), 23233-23241.

646 Wang, X., Liu, F., Tan, W., Li, W., Feng, X. and Sparks, D. (2013) Characteristics of Phosphate Adsorption-
647 Desorption Onto Ferrihydrite: Comparison With Well-Crystalline Fe (Hydr)Oxides. Soil Science 178, 1-11.

648